Supplementary Information

Evaluating the efficacy of zeolites synthesized from natural clay for the methanol-to-hydrocarbons process

Xinyu You,[a] Xin Zhang,[a] Yiru Ye,[a] Hexun Zhou,[a] Shican Jiang,[a] Xue Zhou,[a] Abhishek Dutta Chowdhury*[a]

[a] College of Chemistry and Molecular Sciences, Wuhan University, Wuhan, Hubei, China.

E-mail: abhishek@whu.edu.cn

S1. Materials and Methods

S1.1 Materials

Colloidal silica (LUDOX AS-40, 40wt %, Aldrich), sodium aluminate ($NaAlO_2$, 99.8wt%, Shanghai Macklin, China), Kaolin clay (ASP® G90 by BASF), sodium hydroxide (NaOH, 99.9wt%, Sinopharm Chemical Reagent, China), tetrapropyl-ammonium hydroxide (TPAOH, 40wt % in H_2O, Energy Chemical, China), tetraethy-lammonium hydroxide (TEAOH, 25% in H_2O, Energy Chemical, China), N,N,N-Trimethyl-1-ammonium adamantane (TMAdaOH, 25% in H_2O, Energy Chemical, China), ammonium chloride (NH_4Cl, AR, Shanghai Macklin, China), ammonium fluoride (NH_4F, AR, Shanghai Meryer, China), and deionized water (≥18.25 MΩ·cm under 25°C) were used as received unless stated otherwise.

S1.2 Synthesis of zeolite materials

Pretreatment of Kaolin: Kaolin could typically be transformed into a more readily utilizable metakaolin (amorphous) through various methods, including acid/alkaline treatment and direct calcination.[1–10] Our work employed the simple direct pretreatment method, where kaolin was heated at 800 °C for 2 hours with a heating rate of 10 °C/ min to convert into metakaolin. After the heat treatment at 800°C for 2 hours, its morphology showed no significant changes (**Fig. S1**), and as shown in **Fig. S2**, the characteristic diffraction peaks of kaolin (2θ = 12°, 20°, 26°, and 35°) have mostly disappeared,[5,11] indicating the transformation into amorphous metakaolin phase, which will be utilized for synthesizing zeolites. The Type-II N_2 adsorption/desorption isotherm displayed in **Fig. S6** also indicated metakaolin was a non-

porous material. [12] Referring to the composition of metakaolin in **Table S1**, the chemical formula for pure metakaolin was $Al_2O_3 \cdot 2SiO_2$, with a Si/Al ratio of 1.[13,14] This indicated the BASF kaolin clay contained additional aluminum. Based on the composition of metakaolin, all kaolin-derived zeolite syntheses were attempted to keep SiO_2/Al_2O_3 ratio of around 100. The actual Si / Al ratio is shown in **Table 1** and **Table S2**. (K) zeolite and (R) zeolite represent kaolin-derived and traditionally synthesized zeolites, respectively. Unless otherwise specified, all zeolite samples used for testing, including all (K) zeolites and (R) zeolites, refer to H-type zeolites after ion exchange and calcination. The detailed synthesis procedures were as follows:

Synthesis of (K) SSZ-13 and (R) SSZ-13 zeolites: The metakaolin obtained after the heat treatment and, as a reference material for comparison, conventional $NaAlO_2$, were used as the sole aluminum sources for the hydrothermal synthesis of (K) SSZ-13 and (R) SSZ-13 zeolites, respectively. Herein, N,N,N-Trimethyl-1-ammonium adamantane (TMAdaOH) was used as the organic structure directing agent (OSDA) for synthesizing SSZ-13 zeolite,[15,16] and silica sol served as the silicon source. The gel composition was formulated as follows: 1 SiO_2: 0.2 TMAdaOH: 0.01 Metakaolin: 0.06 NaOH: 6 H_2O. We must report that the SSZ-13 zeolite tends to form other impurity phases in dilute gel systems, thus requiring the evaporation of excess water during gel preparation.[16] Typically, the following synthesis procedure was followed: Deionized water and TMAdaOH (as OSDA) were sequentially added to a 50 ml PTFE container, and the excess H_2O was evaporated under vigorous stirring at 70 °C. After cooling, NaOH and metakaolin (or $NaAlO_2$) were added with a 15-minute interval between them while maintaining continuous stirring. After thorough stirring for 2 hours, silica sol was

rapidly added under stirring and allowed to age for 24 hours further. After completion of the aging step, the PTFE container was placed in a reaction vessel, which was subjected to hydrothermal crystallization in a static oven at 165 °C for 96 hours (4 days). After cooling, the crystallized solution was centrifuged three times with deionized water (at a speed of 9000 rpm). Subsequently, the obtained solid was dried overnight at 90 °C in an oven. The dried sample was then ground into powder and calcined at 500 °C for 6 hours in a muffle furnace (with a heating rate of 10 °C/ min) to obtain the Na-type (K) SSZ-13 and (R) SSZ-13 zeolite samples. Afterward, Na-type (K) SSZ-13 and (R) SSZ-13 zeolites were subjected to two ion exchanges in a 1 mol/L NH_4Cl solution at 80 °C, each lasting 4 hours for a total of 8 hours. The ion-exchanged zeolites were centrifuged with deionized water thrice and dried overnight at 90 °C in an oven. Finally, the obtained solids were calcined at 450 °C for 4 hours in a muffle furnace to obtain the H-type (K) SSZ-13 and (R) SSZ-13 zeolite materials.

Synthesis of (K) ZSM-5 and (R) ZSM-5 zeolites: Similarly, metakaolin and $NaAlO_2$ were used as the sole aluminum sources to synthesize (K) ZSM-5 and (R) ZSM-5 zeolites, respectively. Tetrapropyl-ammonium hydroxide (TPAOH) and silica sol were used as the OSDA and silicon source, respectively.[17] The gel composition was formulated as follows: $1SiO_2$: 0.3 TPAOH: 0.01 Metakaolin (or Al_2O_3): 0.06 NaOH: 30 H_2O. A similar synthesis protocol was used: Deionized water and TPAOH were sequentially added to a 50 ml PTFE container and stirred for 30 minutes. After cooling, NaOH and Metakaolin (or $NaAlO_2$) were added with a 15-minute interval between them while maintaining continuous stirring. After thorough stirring for 2 hours, silica sol was rapidly added under stirring and allowed to age for

24 hours. Once the aging was completed, the PTFE container containing the mixture was transferred to a reaction vessel, which was subjected to hydrothermal crystallization in a static oven at 180 °C for 72 hours (3 days). Following the crystallization process, the resulting solution was centrifuged three times using deionized water at 9000 rpm. Subsequently, the obtained sample was dried overnight at 90 °C in an oven. The dried material was then ground into a powder and subjected to calcination at 500 °C for 6 hours in a muffle furnace, with a heating rate of 10 °C/ min. This process yielded the Na-type (K) ZSM-5 and (R) ZSM-5 zeolite samples. Finally, the ion exchange step, identical to that described for the SSZ-13 zeolites, was followed to yield H-type (K) ZSM-5 and (R) ZSM-5 zeolite materials.

Synthesis of (K) Beta and (R) Beta zeolites: Likewise, (K) Beta and (R) Beta zeolites were synthesized using metakaolin and $NaAlO_2$ as the sole aluminum sources, respectively. It is worth noting that the direct synthesis of high silica Beta zeolite is a challenging matter.[18] Herein, we successfully synthesized it by introducing F^- ions into the synthesis gel using NH_4F. Tetraethylammonium hydroxide (TEAOH) was used as the OSDA, and silica sol served as the silicon source.[18,19] The gel composition consisted of $1SiO_2$: 0.6 TEAOH: 0.01 Metakaolin (Al_2O_3): 0.06 NaOH: 0.2 NH_4F: 12 H_2O. The synthesis procedure was as follows: Deionized water and TEAOH were sequentially added to a 50 ml PTFE container and stirred for 30 minutes. NaOH and metakaolin ($NaAlO_2$) were added at 15-minute intervals while continuously stirring. After 2 hours of thorough stirring, silica sol was rapidly added under stirring conditions and further went for 24 hours to allow aging. NH_4F was added within the last 2 hours before the completion of aging. After aging, the PTFE container was placed in a

reaction vessel, which was subjected to hydrothermal crystallization in a static oven at 145 °C for 7 days. Subsequently, centrifugation, drying, and calcination were performed following the same steps described earlier to obtain the Na-type (K) Beta and (R) Beta zeolites. Finally, the ion exchange process was carried out similarly to SSZ-13 and ZSM-5 zeolites, resulting in the final formation of the H-type (K) Beta and (R) Beta zeolite materials.

S1.3 Catalyst Characterization

Powder X-ray diffraction (PXRD) patterns were acquired on Bruker D8 Advance X-ray diffractometer using Cu-Kα (1.54060 Å) radiation, and operated at 40 kV and 40 mA. In order to optimize the count statistics and peak shape profiles, data collection was carried out in the 2θ range of 5-60° using the step size of 0.01° and scan speed of 5 deg/min and applying a low-angle cutting knife to avoid direct beam heating the detector. The bulk chemical composition analysis was performed via inductively coupled plasma (ICP) measurements obtained in a 700 ICP-OES instrument (Agilent), where the samples were digested in acidic solutions under microwave treatment. Quantitative compositional analysis of metakaolin was performed through X-ray fluorescence spectroscopy (XRF) using the ARL Advant X IntellipowerTM 3600 equipment from Thermo Fisher Scientific, USA. Scanning electron microscopy (SEM) imaging was obtained by Hitachi-SU8010, Japan. The elemental mapping was performed by AZtecone (Oxford Instruments), operated at 200 kV. The particle size distribution was determined by Nanomeasure software (developed by Fudan University, China). N_2 physisorption was performed with an automated gas sorption system Micromeritics ASAP

2460 at -196 °C. The calcined zeolite samples and metakaolin were degassed under vacuum for 6 h at 300 °C before the measurement. The total specific surface area of all zeolite samples was determined using BET method at low relative pressures (P/P_0 = 0.05 - 0.20). The total pore volume was determined at P/P_0 = 0.99, while the micropore volumes and micropore surface areas were evaluated using the t-plot method. Temperature-programmed NH_3 desorption (NH_3-TPD) was measured by BELCAT-B from Micky Bayer Co. Ltd (Japan). 50 mg of sample was used for the test in a 30 mL min^{-1} Ar flow. Prior to the test, the sample was heated to 550 °C and kept for 120 min to remove possible impurities. Afterward, the sample was cooled to 50 °C and exposed to a 30 mL min^{-1} NH_3 flow for 1 h to saturate the surface completely, which was followed by purging with a 30 mL min^{-1} ultrahigh purity He flows to remove any physically adsorbed NH_3 for 30 min. After all these pretreatments, the catalyst was heated from 50 ° to 700 °C at a rate of 10 °C min^{-1}. 1D ^{27}Al magic angle spinning (MAS) solid-state nuclear magnetic resonance (NMR) spectroscopic experiments were performed on Bruker AVANCE NEO 800 spectrometers operating at 800 MHz frequency using the 3.2 mm broadband solid-state probe. The ^{27}Al NMR Chemical shift is referenced according to the test results of $Al(NO_3)_2$. For all ^{27}Al MAS solid-state NMR experiments, 0.5 s recycle delay, and 2048 scans were applied. All NMR spectra were processed and analyzed using Bruker TopSpin 4.0. The deposited coke amount of spent catalysts was determined through thermal gravimetric analysis (TGA) using a STA 449 F3 Jupiter® instrument manufactured by NETZSCH in Germany. Typically, 10 mg of the spent catalysts were heated from room temperature to 900 °C at a rate of 10 °C/min in an air flow of 30 ml/min. (The spent catalysts were obtained by conducting

MTH testing until deactivation, with the specific reaction times provided in the catalytic results of **Fig. S9 to S15**. These TGA characterizations have been performed on sived post-reacted zeolites after the manual removal of SiC.)

S1.4 MTH catalytic tests

Methanol-to-hydrocarbons (MTH) reactions were performed in a fixed-bed reactor (Xiamen Hande Engineering Co., Ltd.) with a 10 mm inner diameter quartz tubular reactor. The calcined zeolite catalysts were pelletized and crushed into 45-110 mesh, and the obtained catalysts (0.5 g) were mixed with SiC (3 g) at a weight ratio of 1:6 (catalyst/ SiC) to dilute catalysts and avoid the formation of hot spots.[20,21] SiC played no catalytic role in methanol conversion reactions. This fact was substantiated through our conducted blank experiments, wherein methanol passed through a reactor filled exclusively with 3g SiC at 500°C and a WHSV of 2 h^{-1} without undergoing any conversion. Before the reaction, the catalytic bed was pretreated with Argon at 550 °C for 2 h. After pretreatment, the temperature decreased to reaction temperature (400-500 °C), and WHSV was set to 2 h^{-1}, with methanol being diluted in Ar to a constant molar MeOH/Ar ratio of 1:2 at a pressure of 1 bar. The reaction products were analyzed online using gas chromatography (GC-8850, Lunan Ruihong Co., Ltd.) with three detectors: two flame ionization detectors (FIDs) and one thermal conductivity detector (TCD). The permanent gas (Ar, N_2, CH_4, CO, and CO_2) was detected by TCD through GDX-104 and TDX-101 columns. The separation of methanol, dimethyl ether (DME), and C_1−C_4 hydrocarbons was carried out on a KB-PLOT Q column (30m*0.53mm*40um), while the

separation of C_{5+} hydrocarbons was carried out on a KB-5 column (60m*0.32mm*1.0um). Methanol conversion (X, %) and selectivity (S, %) of each product are defined as follows:

$$X = \frac{n_{C,MeOH_{in}} - n_{C,MeOH_{out}} - 2 \cdot n_{C,DME_{out}}}{n_{C,MeOH_{in}}} \cdot 100\% \quad (1)$$

$$S_i = \frac{i \cdot n_{Ci}}{n_{C,MeOH_{in}} - n_{C,oxy_{out}}} \cdot 100\% \quad (2)$$

Where C_{MeOHin}, $C_{MeOHout}$, are the concentrations determined by GC analysis of methanol in the blank and in the reactor effluent (unit: mol/L). C_{DMEout}, and C_{oxyout} are the concentrations of DME and oxygenates in the effluents (unit: mol/L), n_{ci} is the molar quantity of product *Ci* in the effluents and *i* is the number of carbon atoms in its molecule.

S1.5 Operando UV/Vis DRS Study Coupled with Online Mass Spectrometry

All the catalytic operando studies were performed using a Linkam cell (THMS600) equipped with a temperature controller (Linkam TMS94), and its lid is equipped with a quartz window compatible with UV/Vis detection. The UV/Vis diffuse reflectance spectroscopy (DRS) measurements were performed with an AvaSpec-ULS2048L-USB2-UA-RS micro-spectrophotometer from Avantes. Halogen and deuterium lamps were used together for illumination. The online gas phase product analyses were performed by Pfeiffer OmniStar GSD 350 O3 (1-200 amu) mass spectrometer, which was directly connected to the outlet of the Linkam cell. The National Institute of Standards and Technology (NIST) mass spectrometry database was consulted for assignment and referencing purposes. Herein, the signals identified

at 26 amu, 41 amu, 43 amu, 56 amu, and 78 amu were attributed to ethylene, propylene, butyl-, butene and benzene, respectively. During operando studies, all reactions were performed without pressing and sieving the zeolite materials. Operando UV/Vis DRS reactions were performed using ca. 40 mg of the catalyst material. Initially, it was placed on the heating stage of the Linkam cell, which was further connected to a water cooler. The inlet of the cell was connected to the N_2 gas line, via a liquid saturator, whereas the outlet was either connected to the Pfeiffer mass spectrometer or vented out. The lid of the Linkam cell is equipped with a quartz window to monitor the reaction by UV-vis DRS. Before each UV-vis DRS, the material was further pre-treated/calcined according to the following procedure under an N_2 environment (flow rate of 20 ml/min): heating to 673 K at 10 K/ min and keeping the sample at this temperature for the next 10min; then, heating the sample to 823 K at a rate of 5 K/ min and hold there for the next 30 min. Next, the sample was cooled down to the reaction temperature (as specified in the figure caption) with a rate of 10 K/ min under a flow of N_2 gas (flow rate of 20 ml/min). The starting time of the reaction was considered when the inward N_2 flow goes through the liquid saturator. Finally, the reaction was quenched by rapid cooling of the Linkam cell using a Linkam TMS94 temperature controller. During these experiments, the UV-vis DRS was recorded every 15 s intervals during the MTH experiment, which typically took 20 min. The Operando UV-vis spectra were collected every minute, with 300 accumulations of 50 ms exposure time each.[20]

S2. Supplementary Figures

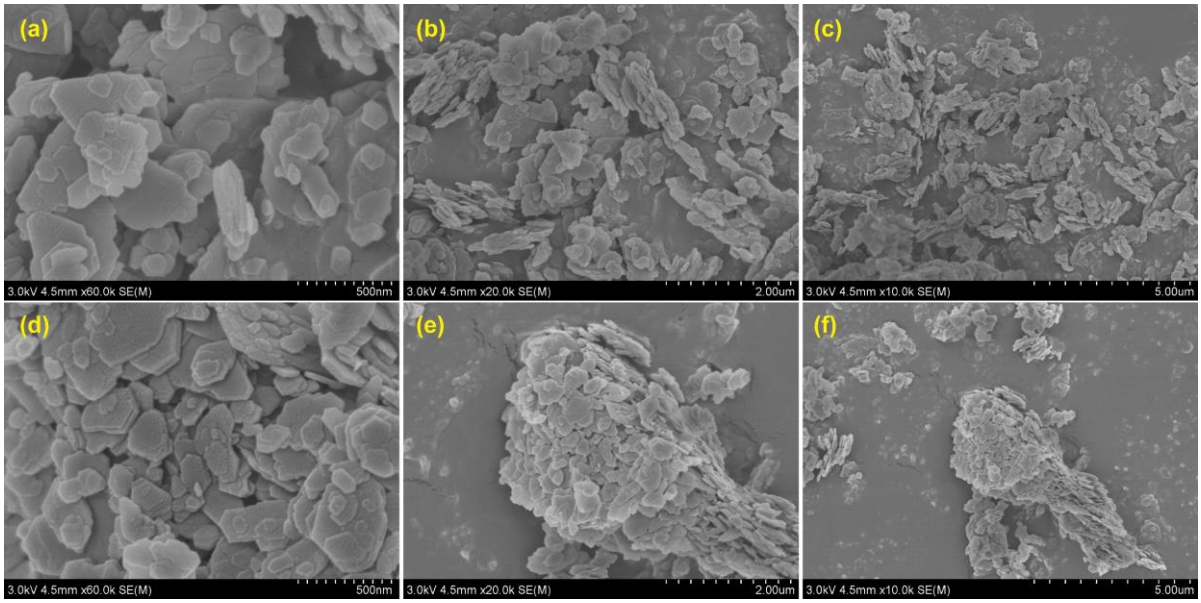

Fig. S1. SEM images of **(a, b, c)** kaolin and **(d, e, f)** metakaolin activated at 800 °C for 2 hours.

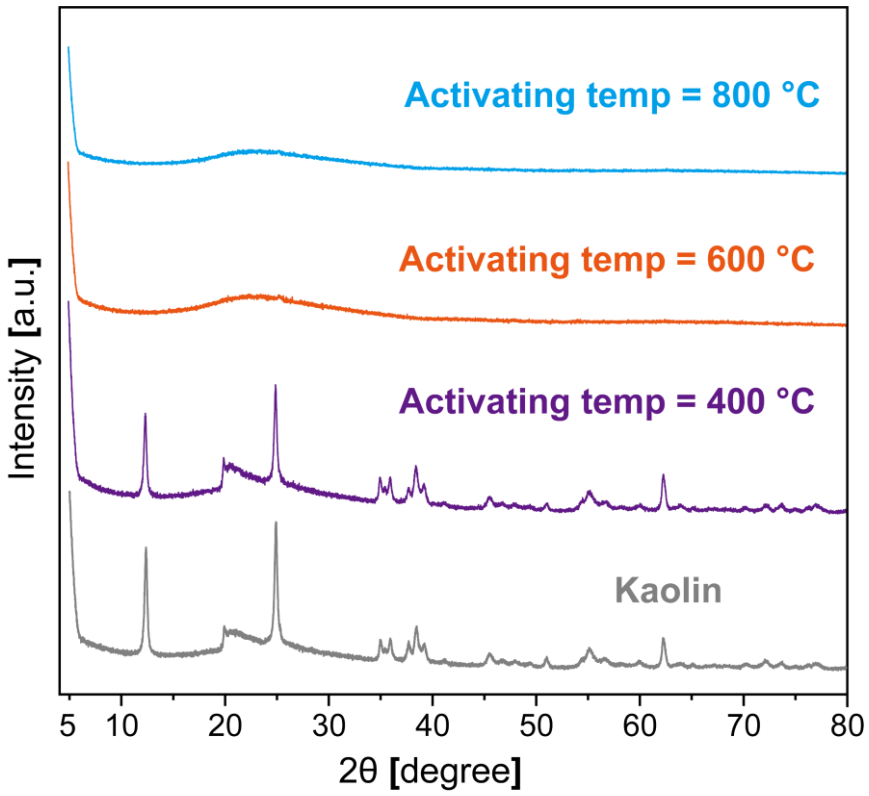

Fig. S2. X-ray diffraction (XRD) patterns of kaolin and metakaolin samples activated at different temperatures.

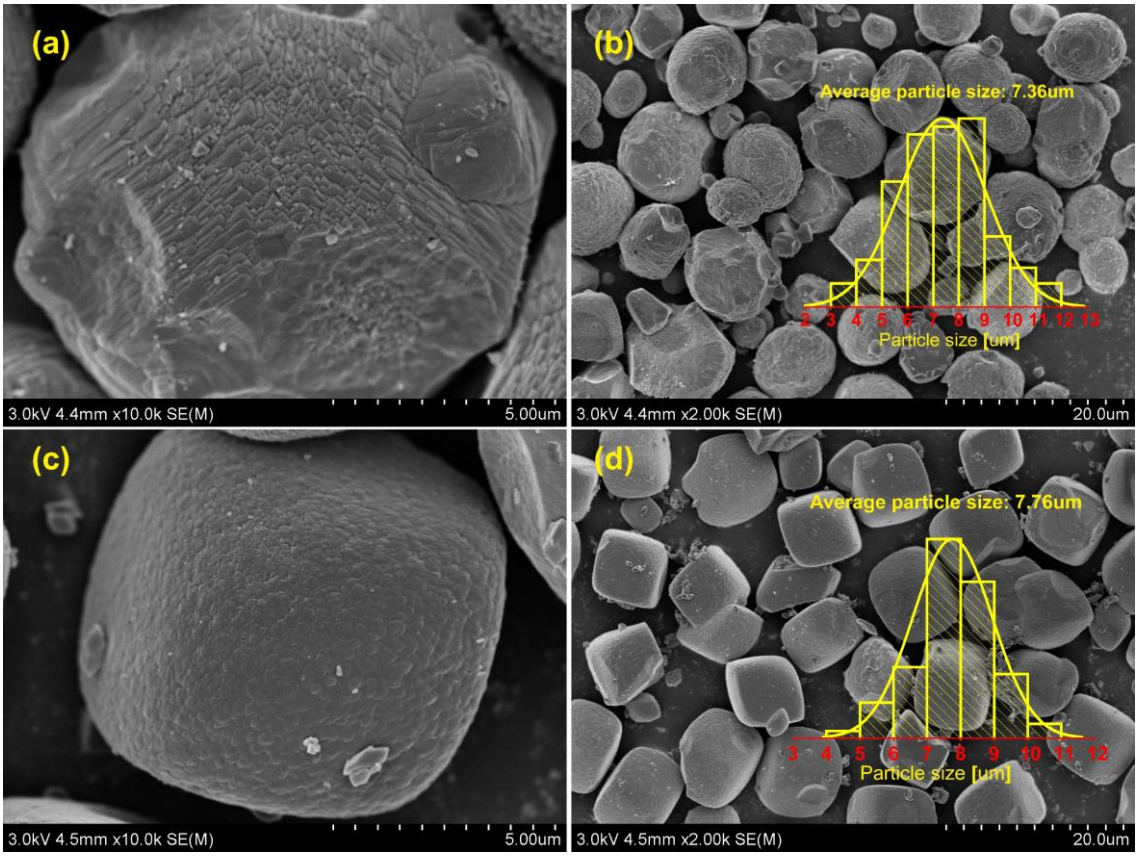

Fig. S3. SEM images of **(a, b)** (K) SSZ-13 and **(c, d)** (R) SSZ-13 zeolites (R and K represent reference and kaolin-derived zeolites, respectively).

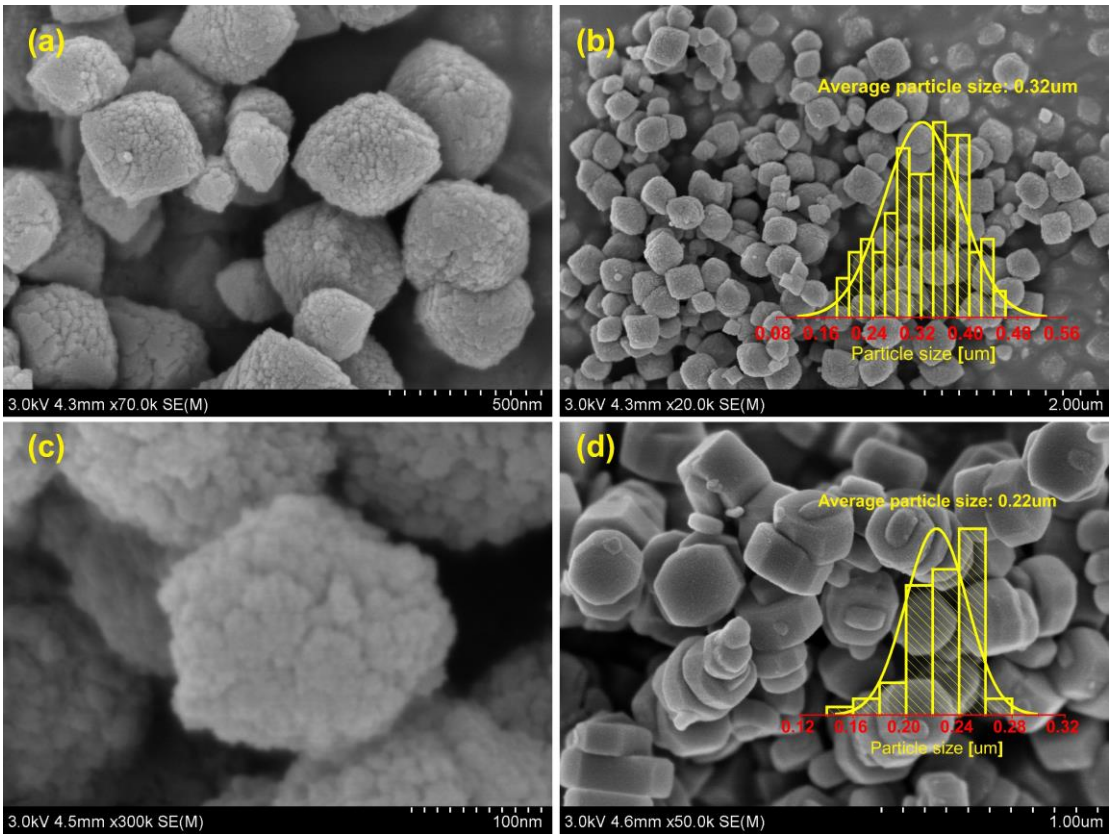

Fig. S4. SEM images of **(a, b, c)** (K) ZSM-5 and **(d)** (R) ZSM-5 zeolites (R and K represent reference and kaolin-derived zeolites, respectively).

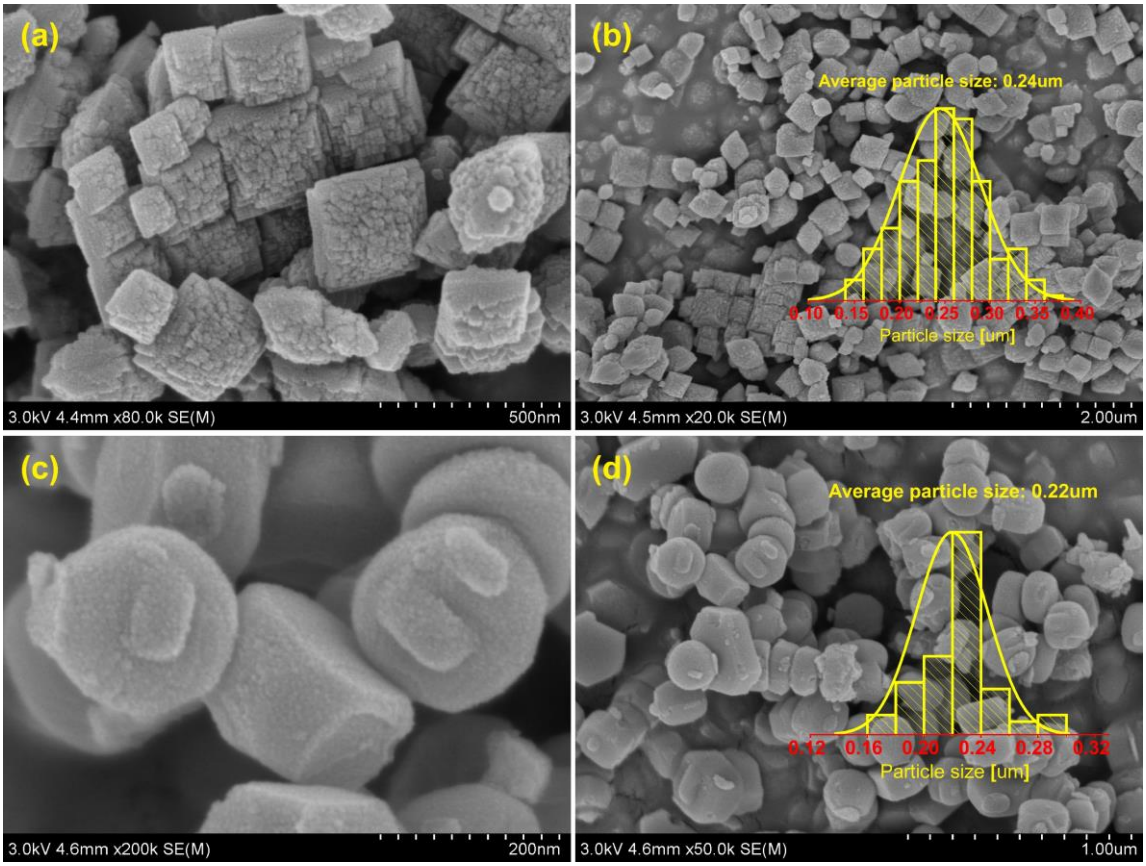

Fig. S5. SEM images of **(a, b)** (K) Beta and **(c, d)** (R) Beta zeolites (R and K represent reference and kaolin-derived zeolites, respectively).

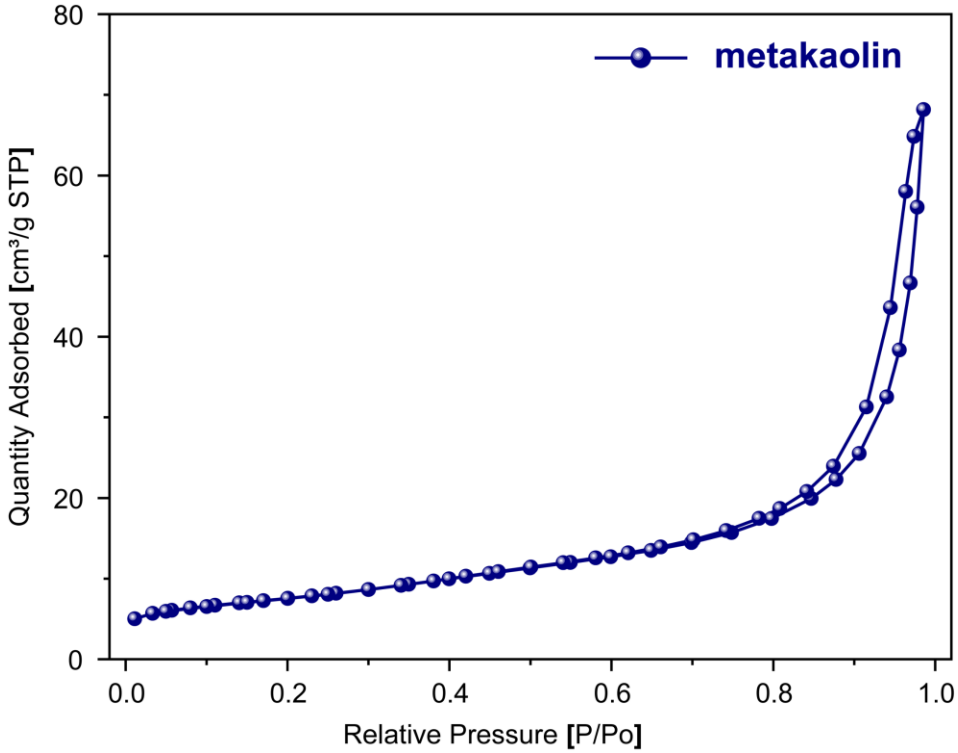

Fig. S6. N_2 adsorption/desorption isotherm of metakaolin (from kaolin activated at 800 °C for 2 hours).

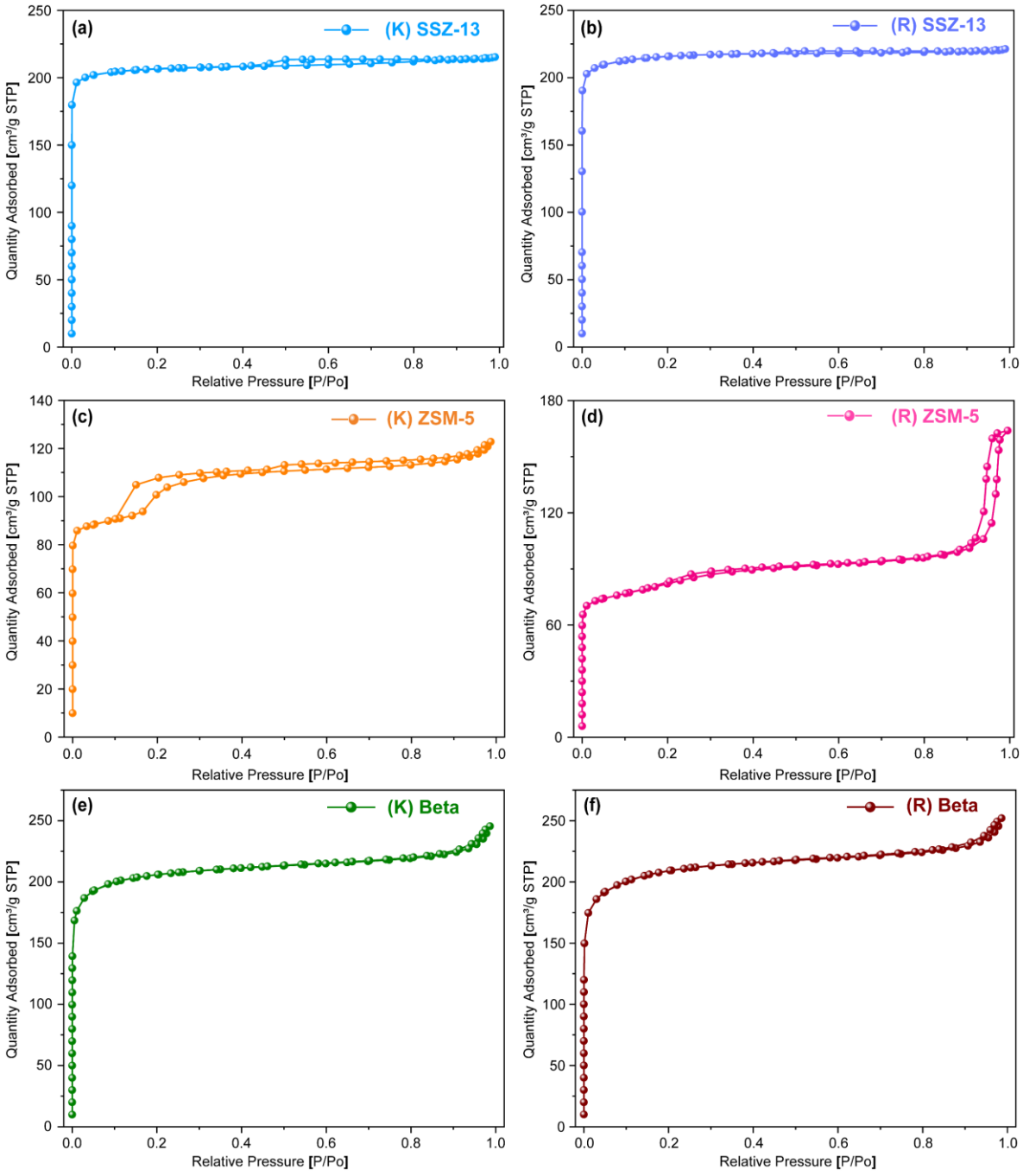

Fig. S7. N_2 adsorption/desorption isotherm of **(a)** (K) SSZ-13, **(b)** (R) SSZ-13, **(c)** (K) ZSM-5, **(d)** (R) ZSM-5, **(e)** (K) Beta and **(f)** (R) Beta zeolites (R and K represent reference and kaolin-derived zeolites, respectively). Also, see **Table 1** for data comparison.

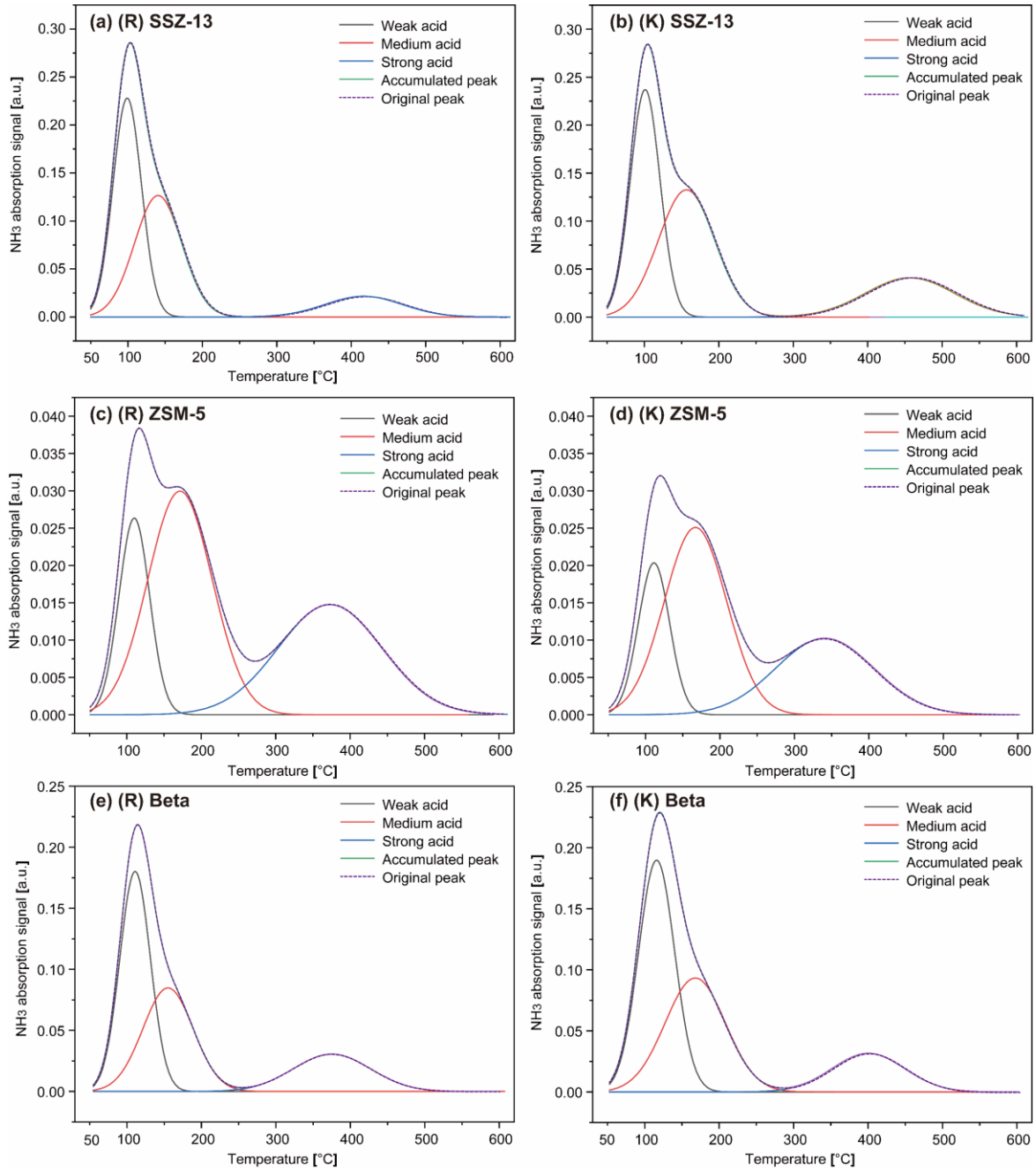

Fig. S8. NH_3-TPD profiles of **(a)** (R) SSZ-13, **(b)** (K) SSZ-13, **(c)** (R) ZSM-5, **(d)** (K) ZSM-5, **(e)** (R) Beta and **(f)** (K) Beta zeolites (R and K represent reference and kaolin-derived zeolites, respectively). Also, **Table 1** for data comparison.

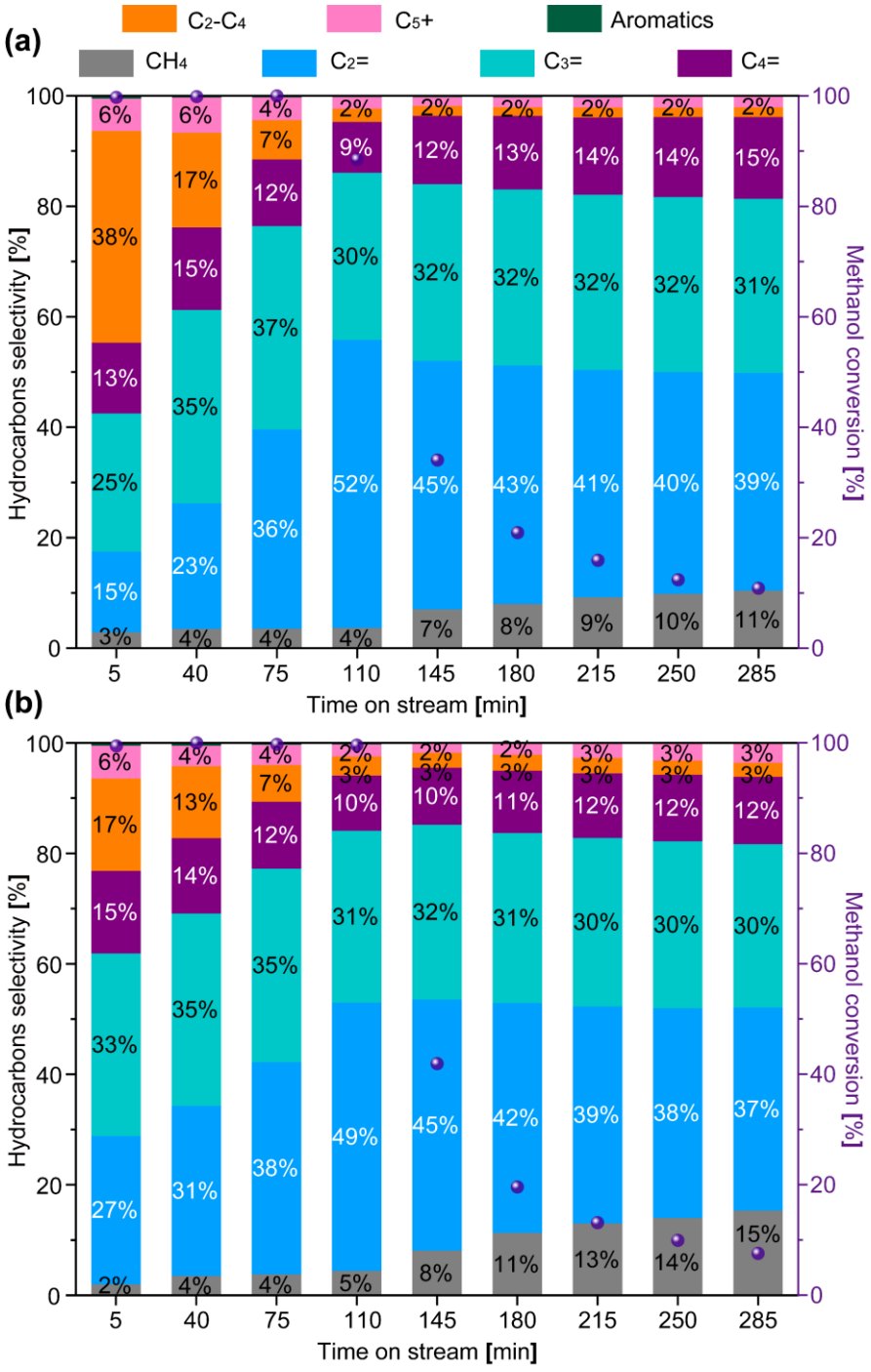

Fig. S9. MTH catalytic test results: Hydrocarbons selectivity over time on stream. **(a)** (K) SSZ-13 and **(b)** (R) SSZ-13 zeolites (WHSV= 2 h^{-1}, reaction temperature = 450 °C) (R and K represent reference and kaolin-derived zeolites, respectively).

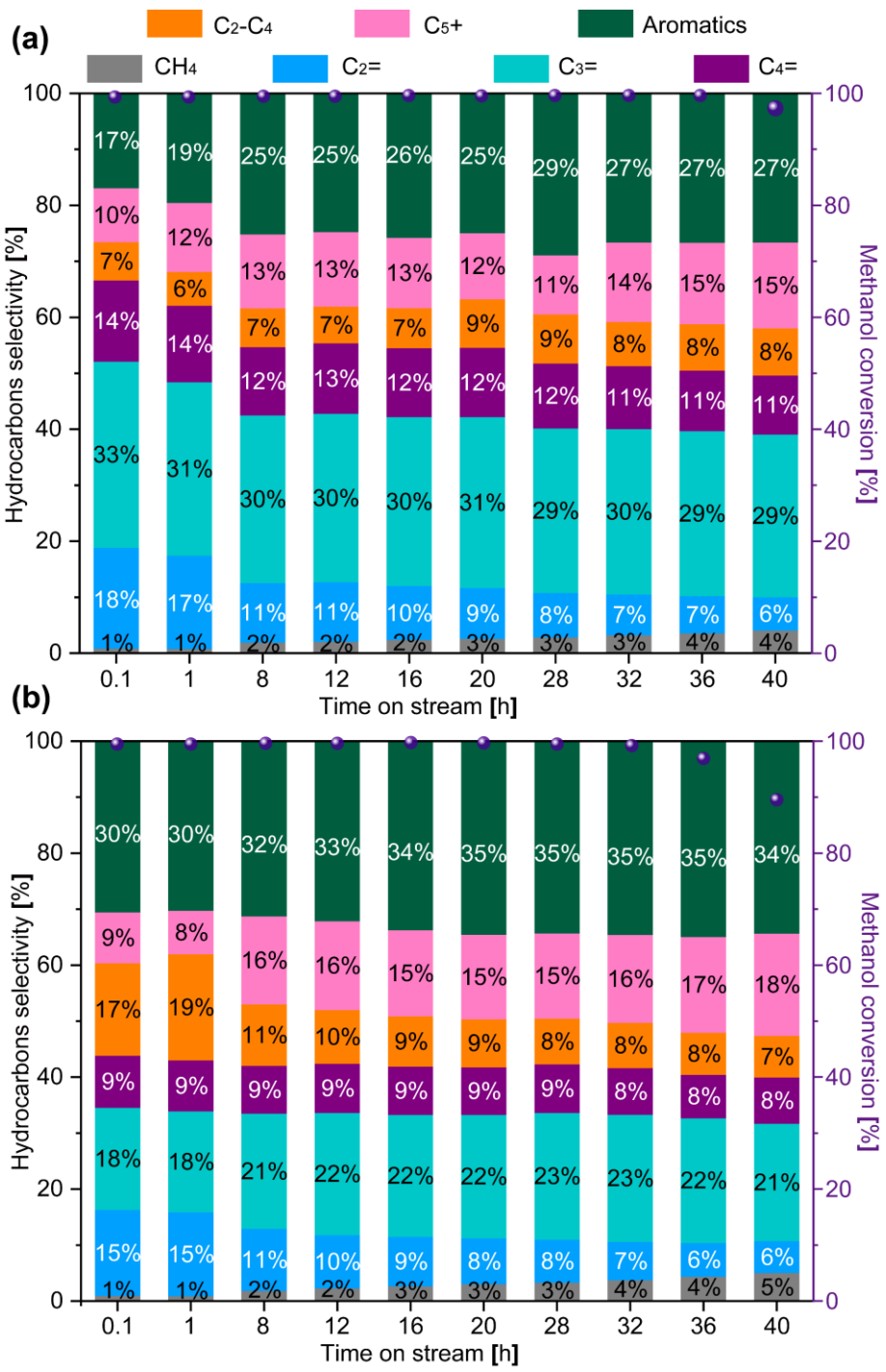

Fig. S10. MTH catalytic test results: Hydrocarbons selectivity over time on stream. **(a)** (K) ZSM-5 and **(b)** (R) ZSM-5 zeolites (WHSV= 2 h^{-1}, reaction temperature = 500 °C) (R and K represent reference and kaolin-derived zeolites, respectively).

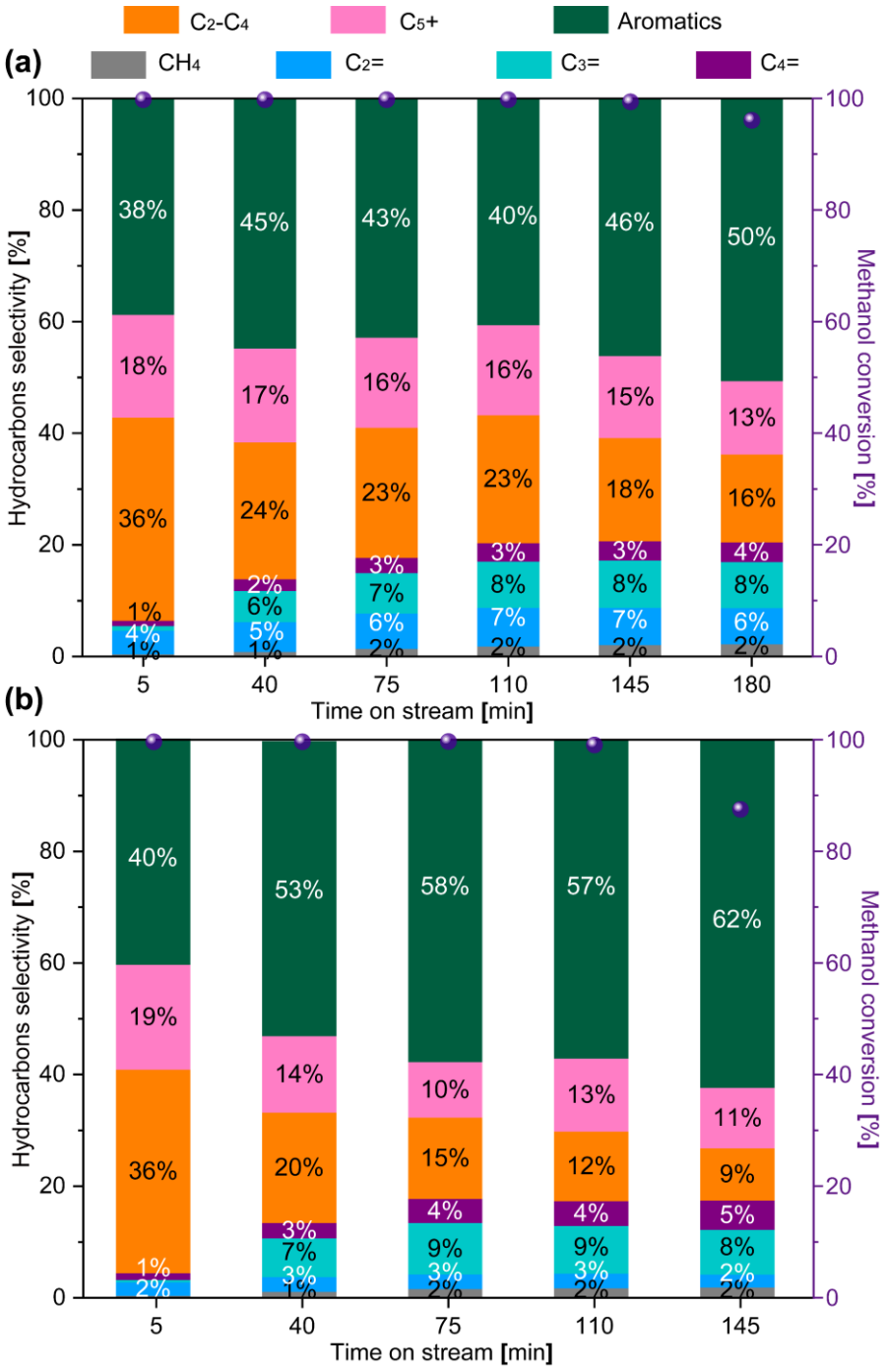

Fig. S11. MTH catalytic test results: Hydrocarbons selectivity over time on stream. **(a)** (K) Beta and **(b)** (R) Beta zeolites (WHSV= 2 h^{-1}, reaction temperature = 400 °C) (R and K represent reference and kaolin-derived zeolites, respectively).

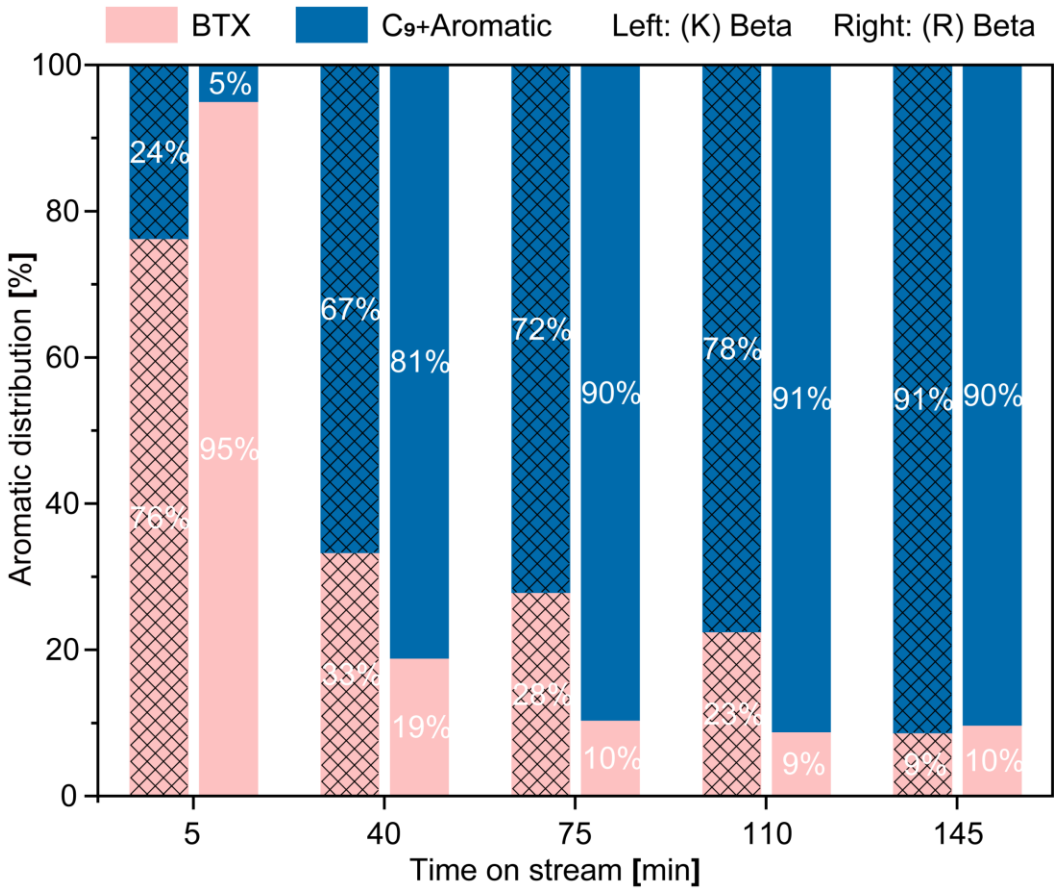

Fig. S12. The BTX (Benzene, toluene and xylene) and C_9^+ aromatic hydrocarbons distribution over time on stream over (K) Beta and (R) Beta zeolites (WHSV= 2 h^{-1}, reaction temperature = 400 °C) (R and K represent reference and kaolin-derived zeolites, respectively).

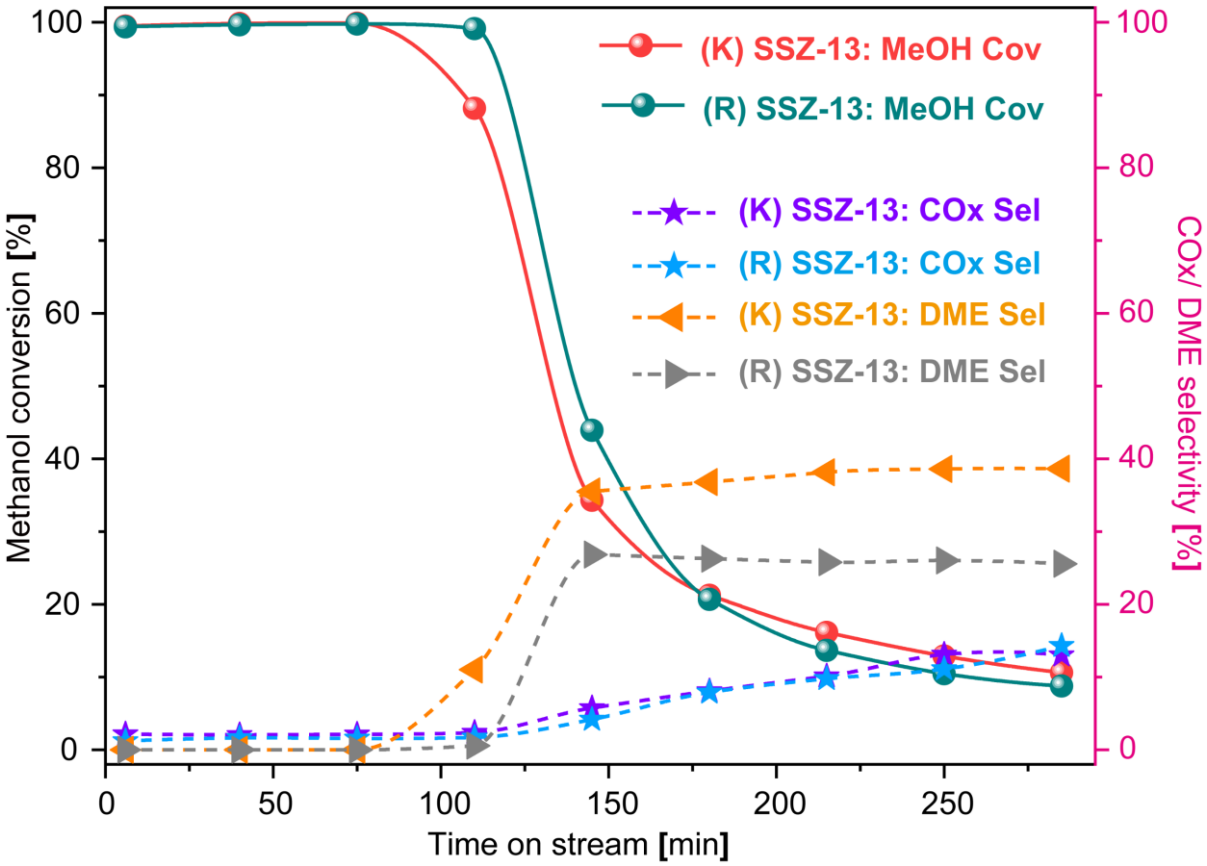

Fig. S13. MTH catalytic test results: the methanol conversion, as well as the selectivity towards COx and dimethyl ether (DME) over time on stream for (K) SSZ-13 and (R) SSZ-13 zeolites (WHSV= 2 h^{-1}, reaction temperature = 450 °C) (R and K represent reference and kaolin-derived zeolites, respectively).

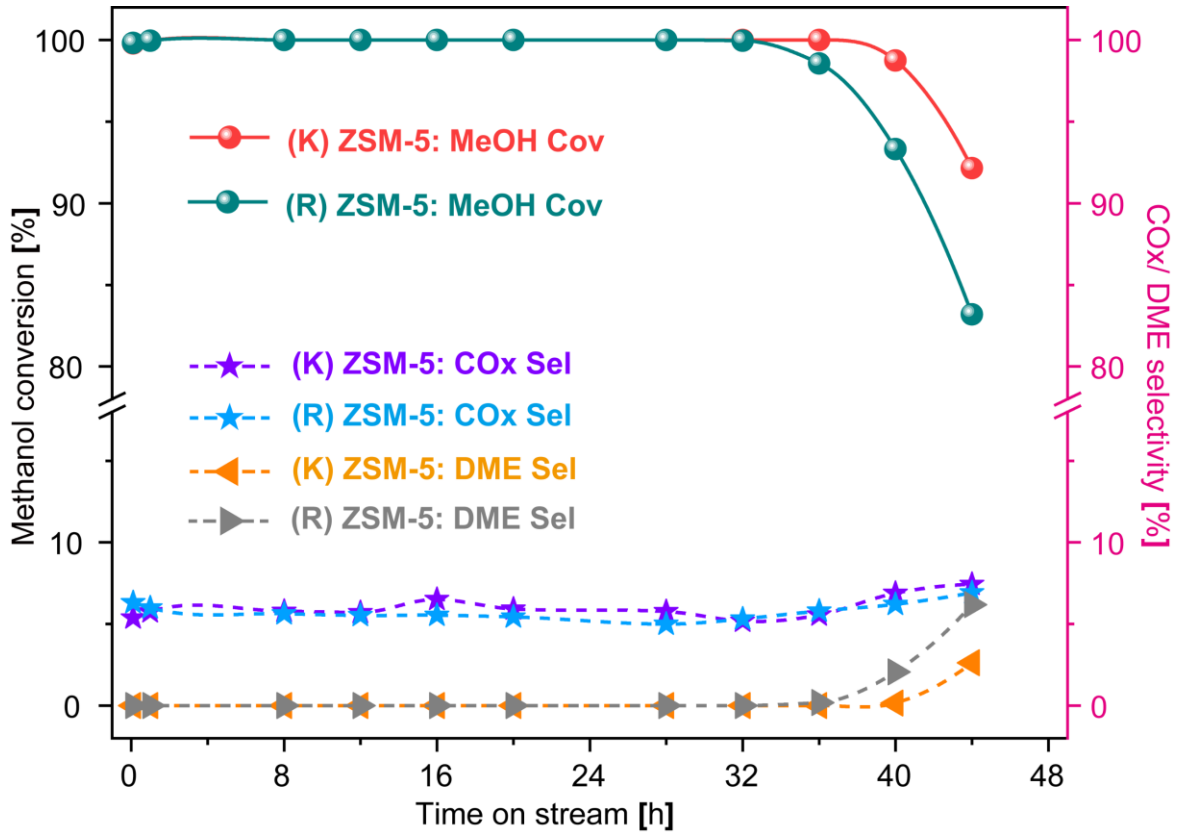

Fig. S14. MTH catalytic test results: the methanol conversion, as well as the selectivity towards COx and dimethyl ether (DME) over time on stream for (K) ZSM-5 and (R) ZSM-5 zeolites (WHSV= 2 h^{-1}, reaction temperature = 500 °C) (R and K represent reference and kaolin-derived zeolites, respectively).

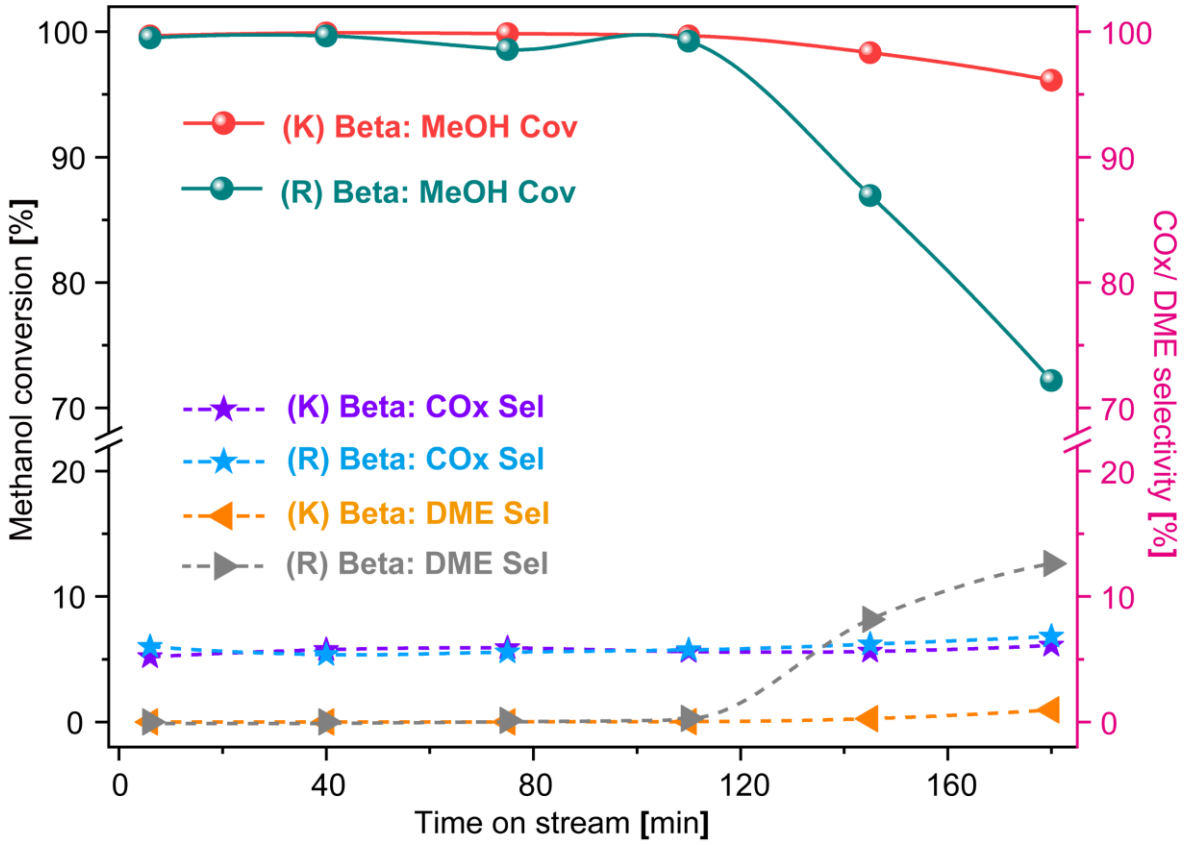

Fig. S15. MTH catalytic test results: the methanol conversion, as well as the selectivity towards COx and dimethyl ether (DME) over time on stream for (K) Beta and (R) Beta zeolites (WHSV= 2 h^{-1}, reaction temperature = 400 °C) (R and K represent reference and kaolin-derived zeolites, respectively).

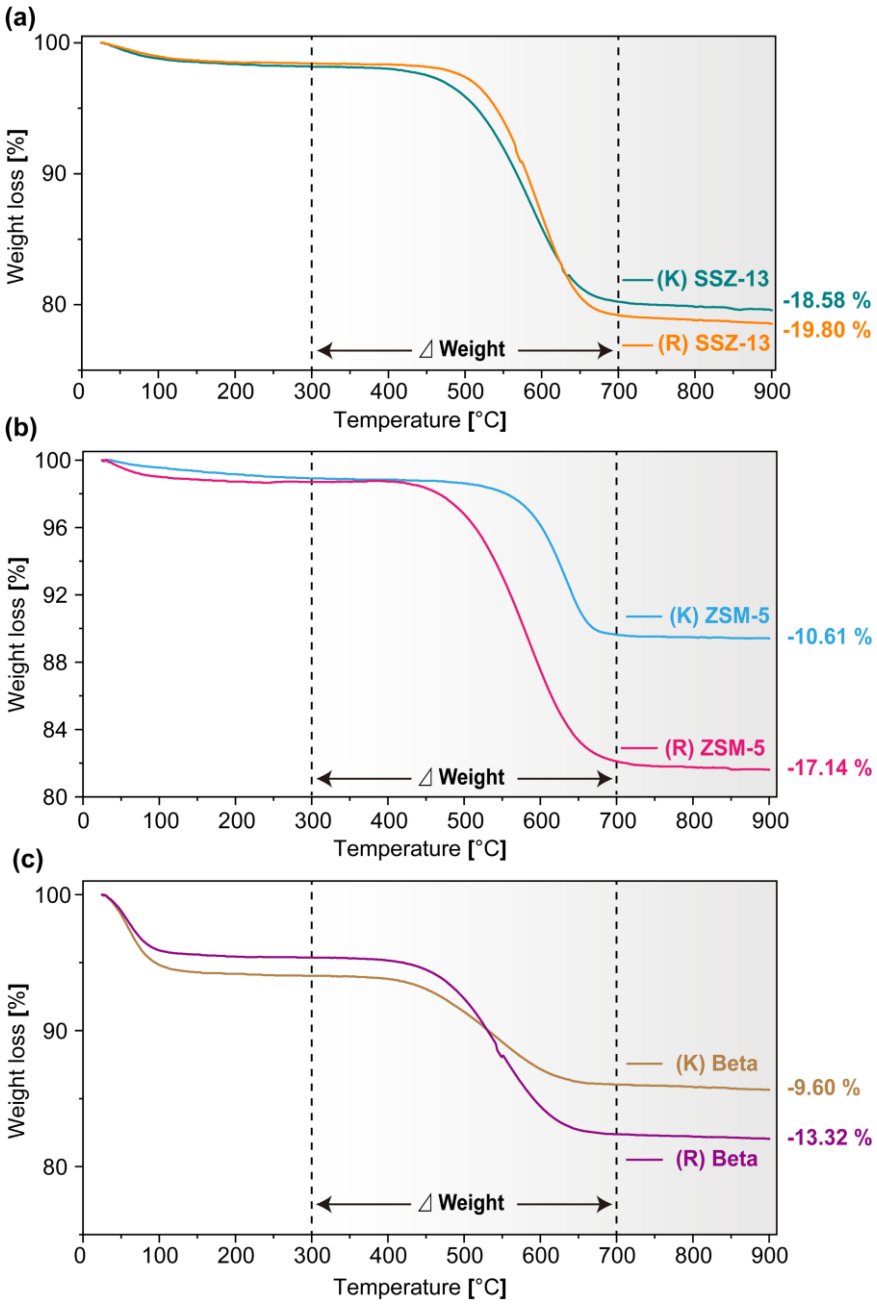

Fig. S16. TGA curves of spent zeolite catalysts obtained after MTH catalytic testing: **(a)** (K) SSZ-13 and (R) SSZ-13 zeolites; **(b)** (K) ZSM-5 and (R) ZSM-5 zeolites; **(c)** (K) Beta and (R) Beta zeolites. These spent and deactivated zeolite catalysts were heated from room temperature to 900 °C at a rate of 10 °C/min in an air flow of 30 ml/min. (R and K represent reference and kaolin-derived zeolites, respectively).

S3. Supplementary Tables

Table S1. Chemical composition of metakaolin. [a]

Analyte	Compound formula	Mass Concentration (%)
Al	Al_2O_3	50.036
Si	SiO_2	47.648
Fe	Fe_2O_3	0.796
Ti	TiO_2	0.687
Na	Na_2O	0.483
P	P_2O_5	0.171
S	SO_3	0.091
Cl	Cl	0.049
Ca	CaO	0.027
Ni	NiO	0.009
	Total	99.97%

[a] Calculated by XRF. The test results have been normalized, and the sum before normalization is 98 %.

Table S2. The Si / Al ratio and main impurity content of kaolin-derived zeolites [a]

Materials	Element mass content (%)				Si/Al
	Si	Al	Fe	Ti	
metakaolin	22.91	25.59	0.213	0.180	0.87
(K) SSZ-13	26.67	0.57	0.009	0.017	46
(K) ZSM-5	27.97	0.42	0.019	0.008	63
(K) Beta	27.72	0.60	0.021	0.015	47

[a] Calculated by ICP. All samples have been dried before testing.

Table S3. A summary of the literature reported MTH catalytic performance over kaolin-derived zeolites.

Refer.	kaolin-source	Types of Zeolites	SiO_2/ Al_2O_3	Reaction conditions	Key products selectivity	Lifetime
22	S-1 type-Kaolin	SAPO-34	0.6	T=450 °C; WHSV=1.73h^{-1}	$C_{2-5}^{=}$: 83 - 90 %	60 mins+
23	Calcined metakaolin	ZSM-5	53	T=450 °C; WHSV=1.5 h^{-1}	$C_{2-4}^{=}$: 48 %;	380 hours
		Hierarchical ZSM-5	48		$C_{2-4}^{=}$: 46 %	70 hours
24	Acid-treated kaolin	c-axis oriented ZSM-5 nanoneedles	19	T=470 °C; WHSV=0.79 h^{-1}	Aromatics: 55 %	430 mins
25	Kaolin microspheres	SAPO-34@Kaolin	0.5	T=450 °C; WHSV=2.5 h^{-1}	$C_{2-3}^{=}$: 80 %	200 mins
26	Kaolin microspheres	SAPO-34	0.65	T=450 °C; WHSV=1 h^{-1}	$C_{2-4}^{=}$: 89.8%	964 mins
27	Calcined metakaolin	ZSM-5	68.79	T=400 °C; WHSV=6.67 h^{-1}	$C_{2-4}^{=}$: 68%	70 hours
28	Calcined metakaolin	Nano-sized ZSM-5 aggregates	25 - 80	T=400 °C; WHSV=6.67 h^{-1}	$C_{2-4}^{=}$: 70%	27 hours
our work	***ASP® G90 by BASF***	***SSZ-13***	***91***	***T=450 °C; WHSV=2 h^{-1}***	***$C_{2-4}^{=}$: 90 %***	***110 mins***
		ZSM-5	***127***	***T=500 °C; WHSV=2 h^{-1}***	***$C_3^{=}$: 30 %***	***40 hours***
		Beta	***93***	***T=400 °C; WHSV=2 h^{-1}***	***Aromatics: 40 - 50 %***	***180 mins***

S4. Supplementary References

1 Y. He, S. Y. He, S. Yin and S. Li, *J. Clean. Prod.*, 2021, **306**, 127248.

2 I. D. R. Mackinnon, G. J. Millar and W. Stolz, *Appl. Clay. Sci.*, 2010, **48**, 622–630.

3 K. Wruck, G. J. Millar and T. Wang, *Environ. Technol. Innov.*, 2021, **21**, 101371.

4 T. Abdullahi, Z. Harun and M. H. D. Othman, *Adv. Powder Technol.*, 2017, **28**, 1827–1840.

5 S. Alonso and A. Palomo, *Mater. Lett.*, 2001, **47**, (1-2), 55-62.

6 J. Q. Wang, Y. X. Huang, Y. Pan and J. X. Mi, *Microporous Mesoporous Mater.*, 2014, **199**, 50–56.

7 S. Chandrasekhar and P. N. Pramada, *Microporous Mesoporous Mater.*, 2008, **108**, 152–161.

8 P. A. Alaba, Y. M. Sani and W. M. A. W. Daud, *Chinese J. Catal.*, 2015, **36**, 1846–1851.

9 S. M. Holmes, S. H. Khoo and A. S. Kovo, *Green Chem.*, 2011, **13**, 1152–1154.

10 P. Pasabeyoglu, G. Moumin, L. de Oliveira, M. Roeb and B. Akata, *J. Clean. Prod.*, 2023, **414**, 137611.

11 Hartati, D. Prasetyoko, M. Santoso, I. Qoniah, W. L. Leaw, P. B. D. Firda and H. Nur, *J. Chin. Chem. Soc.*, 2020, **67**, 911–936.

12 Y. Yue, X. Guo, T. Liu, H. Liu, T. Wang, P. Yuan, H. Zhu, Z. Bai and X. Bao, *Microporous Mesoporous Mater.*, 2020, **293**: 109772.

13 A. Asghari, M. K. Khorrami and S. H. Kazemi, *Sci. Rep.*, 2019, **9**, 1, 17526.

14 D. Hartanto, R. Kurniawati, A. B. Pambudi, W. P. Utomo, W. L. Leaw and H. Nur, *Solid State Sci.*, 2019, **87**, 150–154.

15 X. Zhu, N. Kosinov, J. P. Hofmann, B. Mezari, Q. Qian, R. Rohling, B. M. Weckhuysen, J. Ruiz-Martínez and E. J. M. Hensen, *ChemComm.*, 2016, **52**, 3227–3230.

16 Y. Yang, X. Meng, L. Zhu, J. Yang, G. Zhang, H. Shen and X. Cao, *Inorg. Chem*, 2022, **61**, 21115–21122.

17 H. Sharbini Kamaluddin, X. Gong, P. Ma, K. Narasimharao, A. Dutta Chowdhury and M. Mokhtar, *Mater. Today Chem.*, 2022, **26**, 101061.

18 G. Xiong, M. Feng, J. Liu, Q. Meng, L. Liu and H. Guo, *RSC Adv.*, 2019, **9**, 3653–3660.

19 B. Wang, L. Ren, J. Zhang, R. Peng, S. Jin, Y. Guan, H. Xu and P. Wu, *Microporous Mesoporous Mater.*, 2021, **314**, 110894.

20 Y. Ye, E. Abou-Hamad, X. Gong, T. B. Shoinkhorova, A. Dokania, J. Gascon and A. D. Chowdhury, *Angew. Chem. Int. Ed.*, 2023, e202303124.

21 R. Qi, T. Fu, W. Wan and Z. Li, *Fuel Process. Technol.*, 2017, **155**, 191–199.

22 Z. Jie, C. Yu, N. Zeeshan, W. Yao and W. Fei, *Chin. J. Chem. Eng.*, 2010, **18**, 6, 979-987.

23 L. Xing, Z. Wei, Z. Wen and X. Zhu, *Pet. Sci. Technol.*, 2017, **35**, 2235–2240.

24 K. Shen, W. Qian, N. Wang, J. Zhang and F. Wei, *J. Mater. Chem. A.*, 2013, 1, 3272–3275.

25 L. Zhang, H. Liu, Y. Yue, U. Olsbye and X. Bao, *Catal. Sci. Technol.*, 2019, **9**, 6438–6451.

26 P. Wang, A. Lv, J. Hu, J. Xu and G. Lu, *Ind. Eng. Chem. Res.*, 2011, **50**, 9989–9997.

27 F. Pan, X. Lu, Q. Zhu, Z. Zhang, Y. Yan, T. Wang and S. Chen, *J. Mater. Chem. A*, 2014, **2**, 20667–20675.

28 F. Pan, X. Lu, Q. Zhu, Z. Zhang, Y. Yan, T. Wang and S. Chen, *J. Mater. Chem. A*, 2015, **3**, 4058–4066.